Polymer Bulletin
https://doi.org/10.1007/s00289-021-03574-4

ORIGINAL PAPER

Surfactant-free one-step fabrication of gelatin/PAAm/MWCNT composites for biomedical applications

Berke Düzkan[1] · Bengü Özuğur Uysal[1] · Önder Pekcan[1]

Received: 17 October 2020 / Revised: 20 January 2021 / Accepted: 29 January 2021

Abstract

Well-dispersed multiwalled carbon nanotube (MWCNT) and gelatin-enhanced polyacrylamide (PAAm) composites were synthesized via a free-radical copolymerization method. MWCNTs were added to the composite mixture in various amounts (0.5 mg, 1.0 mg, 1.5 mg, and 2.0 mg) during the nucleation process in order to increase the conductivity. Gelatin/PAAm/MWCNT composites containing different amounts of MWCNTs were then characterized using the ultraviolet–visible (UV–vis) spectroscopic technique to illuminate the dispersibility, and optical properties of the composites. Bandgap energies were evaluated by measuring the absorbance spectra of the composites in a quartz cuvette of the UV–vis spectrophotometer. By calculating the resonance ratio and normalized width values from the absorption response of the composites according to the wavelength, the dispersion rate of the MWCNTs in the composite matrix was determined. The proper ultra-sonication process has been realized so as to maintain the good dispersion of the MWCNTs inside the polymeric matrix lowering the normalized width and increasing the resonance ratio. Polymeric composite materials based on carbon nanotubes are of considerable interest for a variety of biomedical applications. Furthermore, in this work, it is argued that the use of gelatin, another biocompatible material, together with MWCNT makes the properties of the formed composite, suitable for the desired biomedical applications.

Keywords Gelatin · Paam · MWCNT · Tunable bandgap energy · Dispersibility

✉ Bengü Özuğur Uysal
bozugur@khas.edu.tr

[1] Faculty of Engineering and Natural Sciences, Kadir Has University, Cibali, Fatih, 34083 Istanbul, Turkey

Published online: 13 February 2021

Introduction

A number of studies [1–3] have shown that the unique physicochemical and biomedical properties of carbon nanotubes (CNTs) render them an ideal material for production of novel biomimetic materials. The characteristic properties of CNT-based materials and their composites can be exploited to induce good strength, elasticity, and charge transfer properties, and to reinforce biomaterials. Strong, near infrared light absorption capability allows CNTs to be used as efficient photo-thermal agents in biomedical applications. Bone and connective tissue structure implants, laser processing biomedical fighters, artificial muscles, and highly conductive healthcare system electrode layers (defibrillators, cardiographs, encephalographs, etc.) are other particular applications of CNTs in biomedical field [4]. Additionally, the versatile properties render CNTs as a carriage of anticancer drugs, genes, and proteins for chemotherapy [1].

CNTs cannot be used alone in biomedical applications. They must be used together with a flexible host polymer material such as polyacrylamide. Polyacrylamide (PAAm), formed from acrylamide (AAm) subunits, is an organic polymer aggregator which is insoluble in most organic solvents [5]. Because of its physically stable and strong properties, PAAm can be used in many applications [6]. For polyacrylamide gel, the molecular size of the pores is identical to the size of protein molecules. The proteins are therefore filtered through the pores of the gel during electrophoresis, with sizable proteins providing a slower diffusion than the smaller proteins [7]. Polyacrylamide is an atoxic, stable, non-resorbable sterile aqueous gel composed of approximately 2.5% cross-linked acrylamide, non-pyrogenic water and is an important member of the hydrogel family [8]. Hydrogels can differentiate in respect with their equilibrium swelling grade. The hydrogels with high swelling grade show good permeability and biocompatibility [9]. Hydrogels exhibit a human cell-like behavior due to their large amount of water and soft plastic-like structures. Therefore, it contributes greatly to the biocompatibility of hydrogels [10, 11]. Polyacrylamide can also be used to improve the biocompatibility of other natural and synthetic polymers [12]. It is widely used in ophthalmic operations, drug treatment, food packaging products, and water purification [8]. In addition to that, PAAm is a promising hosting organic matrix for composite materials due to its easier shaping, durability and exceptional processability features created with a basic, rehashing, direct chain structure. It can be changed to shape profoundly organized, extended and cross-linked variations [13]. PAAm provides not only mechanical stability and flexibility but also new functionalities after the incorporation of inorganic structures such as CNTs. As a result of the improved interfacial compatibility, the polymer composites incorporating CNT are expected to manifest enhanced mechanical and electrical properties [14]. In addition to the intrinsic properties of the polymer, a further enhancement of biocompatibility, useful properties in electrochemistry, catalysis, and supercapacitors can be possible with the inclusion of CNT into the polymers.

Many researchers use surfactants to ensure that CNT and similar additives are obtained in a homogeneous and well-dispersed form within the polymer host

matrix. Adding even a very small amount of surfactant increases the cost, and it becomes difficult to predict the characteristics of the final product. Therefore, it is vital to use a surfactant-free method. Multiwalled carbon nanotube (MWCNT), special type of CNT, was used as a structural modifier embedded into composite materials by many research groups. Although higher concentrations of surfactants typically help achieve homogeneity of MWCNT suspension, it should not be ignored that such loadings are impractical for larger incorporation of MWCNT into composite materials [14]. Furthermore, surfactants are high-cost and the carbon nanotube grains come together in unsuitable preparation conditions to form larger grains and can agglomerate. The final product desired to be of high quality is negatively affected. The nano-filler dispersion affects suspension quality. Therefore, the dispersion and incorporation of CNTs in polymer matrices are vital. The preparation of CNT embedded polymer composites is a challenging task [15–19]. Many groups have tried to obtain well-dispersed CNTs in polymer matrix by a sonication process using ultrasound shaker because of the shear force generated inside the bath just after standard stirring [20–23]. It was verified by Liao et al. that realizing the proper ultra-sonication method generally results in good dispersion of nanotubes and results in better composite mechanical properties [24]. There has been extensive research on CNT dispersion quality with respect to CNT dispersion, suspension, and sonication settings [25].

Additionally, other groups have shown to provide an ideal environment for cell growth and developing peculiar technology by replacing the commonly used metal bone fracture repair devices and biodegradable, biocompatible scaffolds for bone tissue engineering using gelatin, chitosan, hydroxyapatite, MWCNT, and then shaping them into a real bone [26]. Composite films of gelatin/MWCNT have been prepared by dissolving carbon nanotubes in solutions of aqueous gelatin. It was found that the highly significant increase in mechanical strength may be attributed to well-dispersed nanotubes and good adhesion between them in the gelatin matrix. The opacity of the gelatin film was increased by MWCNT particles which were located in the gelatin matrix, most likely caused by light scattering effect of CNTs. The improved water binding capacity, water permeation, mechanical, and light barrier properties as well as antibacterial activity suggest a great potential of biodegradable and biocompatible Gelatin/MWCNT nanocomposite films in applications such as biomedicine, food, and beverage packaging [27]. A conductive nanocomposite hydrogel has also been developed consisting of oxidized multiwalled carbon nanotubes and polyacrylamide. The CNTs can be uniformly dispersed in the presence of gelatin through hydrogen bonding in the PAAm–CNTs hydrogel. The hydrogel's fundamental network structure is the chemically cross-linked PAAm. Besides, the interactions between the CNTs, gelatin and PAAm chains have indeed led to the hydrogel's high efficiency. The developed hydrogel incorporates adequate stretchability with sensing range higher than 700%, high tensile strength of 0.71 MPa, quick recovery performance (90%) and better sensing capabilities [28]. Gelatin is a biocompatible material [29]. The effect of cross-linker functionality on ocular biocompatibility of chemically modified gelatin hydrogels was investigated by Lai [30]. In vivo biological responses to the gelatin sponges were assessed in subcutaneous Sprague–Dawley rat models by Yang et. al. [31].

Gelatin/CNT [27] and PAAm/CNT [32] composite combinations have been tried and sensitivity, self-recovery property, stretchability [28], the water solubility, water swelling, water uptake [26], water vapor permeability, mechanical [33, 34], and antibacterial properties of the films have been examined so far [26]. However, there is no detailed study on the homogeneity of these composite materials which affects all characteristics and that is crucial for the biomedical applications in terms of their optical properties.

In this study, surfactant-free method was used for manufacturing the composite. After the magnetic stirring, the ultra-sonication process was carried out for all composites in ultrasonic bath in order to have a well-dispersed composite material. Gelatin/PAAm/MWCNT composites containing different amounts of MWCNTs were prepared and characterized using the UV–vis spectroscopic technique to illuminate the dispersibility, and the optical properties of the composites. In this way, the homogeneity and uniformity of the sample can be determined by using only the absorbance data and resonance ratio technique for Gelatin/PAAm/MWCNT composites with surfactant-free preparation instead of extremely high-cost SEM and TEM measurements, which are used to observe and detect agglomeration and inhomogeneity in the sample. Bandgap energies were evaluated by measuring the absorbance of composites in a quartz cuvette of the UV–vis spectrophotometer. Such biocompatible polymeric matrix reinforced with MWCNT composite materials can be used as a structural material for implants, compounds of biological tissues, artificial muscles, and so forth.

Experiment

Materials

Gelatin from porcine skin gel strength 80–120 g Bloom, Type A was purchased from Sigma-Aldrich. Multi-walled carbon nanotubes (MWCNTs, Outer diameter 20–40 nm, Length: 10–30 μm) were purchased from www.cheaptubes.com. Acrylamide (AAm), Ammonium persulfate (APS), *N,N′*-methylenebis-acrylamide (BIS), *N,N,N′,N′*-tetramethylethylenediamine (TEMED) were purchased from Sigma-Aldrich. Distilled water prepared by Chemistry Laboratory of KHU was used as the reaction solvent.

Preparation of gelatin/PAAm/MWCNT composites

About 500.0 mg AAm monomer was dissolved in 5 ml distilled water by stirring them magnetically and mechanically. MWCNT with various amounts (0.5 mg, 1.0 mg, 1.5 mg, and 2.0 mg) was dissolved inside the gelatin solution. MWCNT-gelatin solution and 30.0 mg BIS were added into the beaker inside the ultrasonic bath with 40 kHz, respectively. The ultra-sonication process was performed for 1.5 h so as to homogenize the CNT structures inside the gel. Then, 8.0 mg APS and 5.0 μl TEMED were added to the solution. All gels were prepared at room temperature

(24 °C, Humidity: 40%). Since TEMED was used as accelerator, after dropping TEMED, solutions were immediately taken to the quartz cuvette right before gelation started. Thus, Gelatin/PAAm/MWCNT composites were prepared by the free-radical crosslinking copolymerization (FCC) technique. Then, the quartz cuvette was placed to the measurement cabin of the UV–vis spectrophotometer. According to Dassios et.al. [35] for a homogeneous distribution of 0.5 g of carbon nanotubes in a 1000 mL aqueous suspension, an ultrasound vibrational energy input rate of 7700 J/min over a duration of 90 min is appropriate. For the assessment of the dispersion quality, the polydispersity index, PDI value of each distribution has been used; principally, index values greater than 0.5 are considered to be correlated with polydisperse/nonhomogeneously distributed samples.

The PDI values dropped from 0.7 and 1.25 for 30 and 60 min of ultra-sonication, respectively, to an acceptable 0.5 for a sonication duration of 90 min. The index value that does not change considerably with further energy transmission to the suspension. Imposing an energy density rate of 7.7 J min^{-1} mL^{-1} for a sonication duration of 90 min can be regarded as sufficient for achieving homogeneity in the aqueous suspensions of the investigated MWCNTs [36]. Therefore, in this study, the ultra-sonication time duration was set as 90 min (1.5 h), and the ratio of MWCNT/liquid was selected below 0.0005 g/ml.

Characterization

The variation of the transmitted light intensity during the gelation of Acrylamide with various amounts of MWCNT was measured using Labomed Spectro 22 UV–vis Spectrophotometer in the spectral range of 190–1100 nm wavelengths. The calculations of under the curve area, full-width of half maximum of the absorbance data were performed by Origin 8.0 Software focusing the absorbance data in the range of 190–400 nm wavelengths. The optical bandgap energies of the composites with various MWCNT amounts were calculated from the extrapolation of the absorbance onset.

Results and discussion

Optical studies: Absorbance and transmittance

The Labomed Spectro 22 UV–vis Spectrophotometer used in the experiments allows measurements at only one wavelength. After the gelation process, absorbance and transmittance measurements are taken for single wavelength one by one. Absorbance and transmittance are measured after the calibration for each wavelength. The accuracy of the values was checked with the following well-known formulation [37] between these two quantities.

$$A = 2 - \log 10\,(\%T) \tag{1}$$

Here, A is the absorbance, T is the transmission (percentage transmittance). As seen in Eq. 1, the absorbance has a logarithmic relationship to the transmittance.

Figure 1 depicts the transmittance behavior of Gelatin/PAAm/MWCNT composites with different amount of MWCNT. Transmittance curves of the composite material containing different amounts of MWCNT can be divided into two regions as short wavelength region (Region I) and long wavelength region (Region II). The optical properties of the composite material differ in these two regions. It appears that the opacity of the material is promoted by the increase in the amount of MWCNT. Whereas the composite materials give a low-transmission response to the ultraviolet light in Region I, it is observed that the composite materials remarkably absorb UV light. In Region II, all composite materials are highly translucent. The fact that they have high transmittance values in the visible region is in agreement with the photographs taken just after the gelation of the composite materials placed in the quartz cuvettes (Fig. 2). As expected, the composite material containing 0.5 mg MWCNT has a lighter color than the composite containing 1 mg MWCNT. However, when the MWCNT amount is increased a little more and made 1.5 mg, it is seen that the composite material in the quartz cuvette is relatively more transparent. About 2 mg MWCNT-doped composite has a darker appearance. When the composite with 2 mg MWCNT in the quartz cuvette in Fig. 2d was turned upside down and photographed, Fig. 2e was obtained. All images in Fig. 2 are photographs of the composites in the form of solidified gel. Figure 2d and e prove the full gelation of composites and well-dispersed MWCNT doping. These observations are in agreement with the transmittance curves of the composites in Region II (Fig. 1).

The inclusion of MWCNTs in gelatin/PAAm composites are expected to result in an increase in the absorbance and opacity of the composite materials. According to Fig. 3, absorbance intensity and peak location (wavelength corresponding to

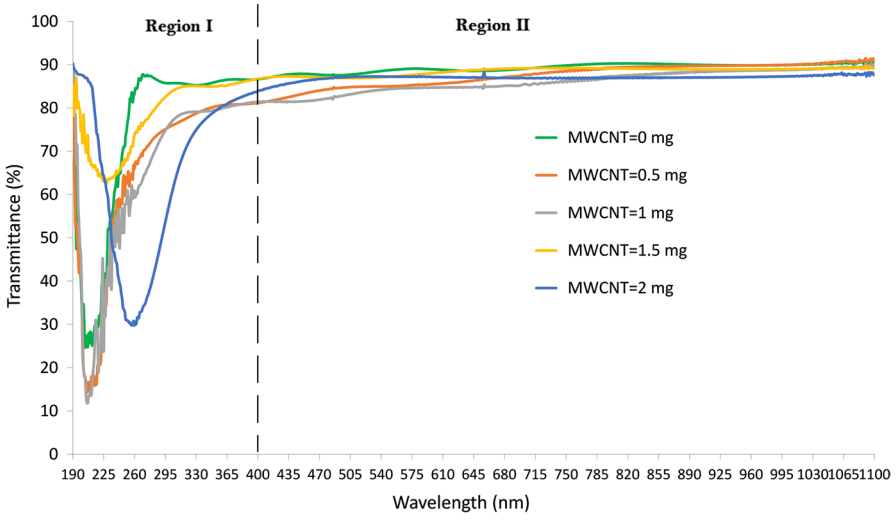

Fig. 1 Transmittance of Gelatin/PAAm/MWCNT composites with various MWCNT amounts: 0, 0.5, 1, 1.5, 2 mg

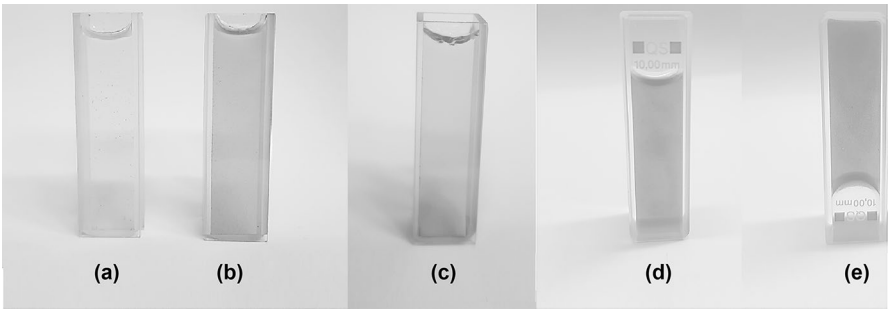

Fig. 2 Photograph of Gelatin/PAAm/MWCNT composites with various MWCNT amounts: **a** 0.5 mg; **b** 1 mg; **c** 1.5 mg; **d** 2 mg

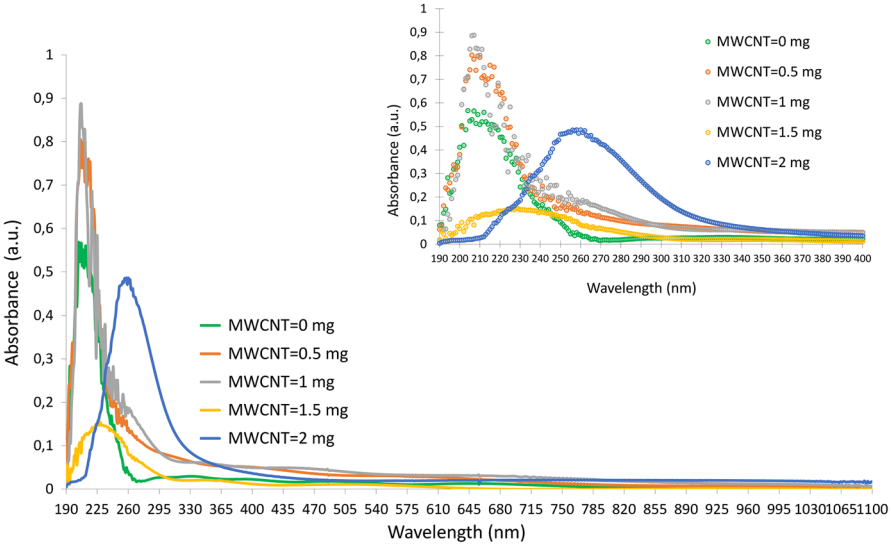

Fig. 3 Absorbance of Gelatin/PAAm/MWCNT composites with various MWCNT amounts: 0, 0.5, 1, 1.5, 2 mg. Inset allows to focus on the ultraviolet light response of composites and to determine absorbance onset wavelength and bandgap energy

the maximum absorbance) values for MWCNT = 0, 0.5, and 1 mg have almost the same form. These peak locations were observed to be smaller than the value around 253 nm which was measured for MWCNTs by other groups [38]. Gelatin/MWCNT absorbance peak is located at 440 nm wavelength [27]. Here, PAAm dominated since it is the highest amount of PAAm in the content of the composite material. So, the peak location for Gelatin/PAAm/MWCNT composites is near 210 nm. PAAm and gelatin composite materials typically appear transparent and colorless. With the inclusion of MWCNT, these properties of composites are lost. As the MWCNT amount increases from 0 to 1 mg, the composite material becomes less transparent (Fig. 1). As seen in Fig. 3, these composites manifest high absorbance values

between the wavelengths of 200 nm and 230 nm in that protein-based materials with high content of aromatic amino acids which absorb UV light [39]. Thus, these composites prevent UV-induced lipid peroxidation [40] and postpone the oxidation caused by light for food and biomedical applications; and/or they can be used as packaging materials [41].

The UV–vis absorbance spectra in Fig. 3 are used to determine the absorbance onset and to calculate the bandgap energy (E_g), using famous Planck–Einstein equation between photon energy, E and wavelength, λ:

$$E = hc/\lambda \tag{2}$$

Here, h is known as Planck constant, and c is the speed of light. If the extrapolated onset value of the absorbance curve (cut-off wavelength) according to the long wavelength is taken as the wavelength λ in Eq. 2, energy, E can be produced as bandgap energy, E_g [42]. Inset in Fig. 3 provides to focus on the absorbance data in the range of 190–400 nm wavelengths which corresponds to the ultraviolet light region, and determination of absorbance onset wavelengths and bandgap energies become possible. Bandgap energies of the composites calculated from the absorbance onset wavelength are listed in Table 1. Narrow bandgap energy can be attributed to high electrical conductivity of the material [43]. The changes in the MWCNT amount inside the composite lead to strong quantum confinement effect with tunable absorbance onset and bandgap energy in a wide wavelength range.

Absorption coefficient and tauc plot

Absorbance A and absorption coefficient α are all measures of the ability of a medium to absorb light (photons). Consider monochromatic light transmitted through a solution, with an incident intensity of I_o and a transmitted intensity of I. Using the Beer–Lambert law [$I = I_o \exp(-\alpha L)$] and the definition of absorbance [$A = \log_{10}(I_o/I)$], it is easy to derive that

$$\alpha = [A \ln(10)]/L, \tag{3}$$

, where L (the unit is meter) is the optical path length of a homogeneous medium for a collimated light beam [44]. For bulk samples L is the thickness of the material. In this study, composite material contains both gelatin and PAAm. Therefore, it is possible to apply both film and bulk material laws to this new composite system. L is taken as 1 cm which is the width of the quartz cuvette.

The optical bandgap (E_g) of Gelatin/PAAM/MWCNT composites can be determined using the Tauc's relation [45] given in Eq. 4, where α is the linear portion of the absorption coefficient, hν is the photon energy and B is a constant.

$$(\alpha h\upsilon) = B\left(h\upsilon - E_g\right)^r \tag{4}$$

A Tauc plot presents the quantity of $h\nu$ on the abscissa and the quantity of $(\alpha h\nu)^{1/r}$ on the ordinate. The resulting plot has a distinct linear regime which denotes the onset of absorption. Thus, extrapolating this linear region to the abscissa yields the

Table 1 Absorbance peak wavelength, intensity and calculates bandgap energies of all composites using absorbance onset wavelength and Tauc's plot

MWCNT amount in Gelatin/PAAm/MWCNT composite (mg)	Absorbance peak wavelength (nm)	Absorbance peak intensity (a.u.)	Bandgap energy (eV, from Absorbance Onset)	Bandgap energy (eV, Direct transition)	Bandgap energy (eV, Indirect transition)
0	212	0.551	4.679	5.261	4.457
0.5	210	0.802	4.882	5.261	4.748
1	211	0.888	4.593	5.372	4.459
1.5	230	0.163	3.875	4.085	3.394
2	260	0.486	3.647	4.092	3.321

energy of the optical bandgap of the material. The value of the exponent r denotes the nature of the transition: $r=1/2$ for direct allowed transitions, $r=3/2$ for direct forbidden transitions, $r=2$ for indirect allowed transitions, $r=3$ for indirect forbidden transitions.

The variation of the bandgap energy values according to the MWCNT amount in Table 1 demonstrates that for the calculation made from absorbance onset and indirect transition, the bandgap energy value of the composite material without MWCNT is lower than the composite material with 0.5 mg MWCNT. When the composite containing 0.5 mg MWCNT is compared with the composite containing 1 mg MWCNT, a decrease in the bandgap energy is observed. Figure 4 shows the Tauc plots of all composites for the direct and indirect allowed transitions. For the direct transition, composites with 0 mg and 0.5 mg MWCNT have the same bandgap energy value; however, the bandgap energy value for 1 mg MWCNT composite is increased. This trend continues for composites with higher MWCNT amounts. This means that the bandgap energy values calculated from the absorbance onset and calculated according to the indirect transition change in line with each other. In other words, it could be concluded in light of these results that this composite material, which anyone formerly did not know whether having direct or indirect transition, exhibits indirect transition.

Dispersibility of composites

The calculations of under the curve area, full-width of half maximum of the absorbance data are employed by using the absorbance–wavelength data of composite with 1.5 mg of MWCNT as presented in Fig. 5. The optical bandgap energies of the composites with various MWCNT amounts are calculated from the extrapolation of absorbance onset. Table 1 summarizes the absorbance peak wavelength, intensity and bandgap energies of all composites. There is a small increase in the absorbance intensity values, while there is no significant change in the cut-off wavelength and the bandgap energy, which is the indicator of the conductivity mechanism. The calculated bandgap energies are in the range of 4.593–4.882 eV (see Table 1). Therefore, one may conclude that the conductivity of the composites does not change significantly for the MWCNT amount between 0 and 1 mg.

In order to prove that the ultra-sonication process is necessary for the production of homogeneous composites, Tan and Resasco [46] have succeeded in mathematically modeling the dispersion state, which is a measure of homogeneity, using the absorbance curve. As stated in this method, the sharpness of the spectral features relative to the background can be quantified by two parameters. The first one called "resonance ratio" is the ratio of the resonant band area to its nonresonant background. The second parameter called "normalized width" is the ratio of the width of the band at half-height to the peak height on a spectrum. These two ratios were used to quantify the effect of different factors in the dispersion procedure. Figure 6 illustrates the absorbance–wavelength plots of all composites by means of these parameters, and aforementioned ratios are calculated and listed in Table 2.

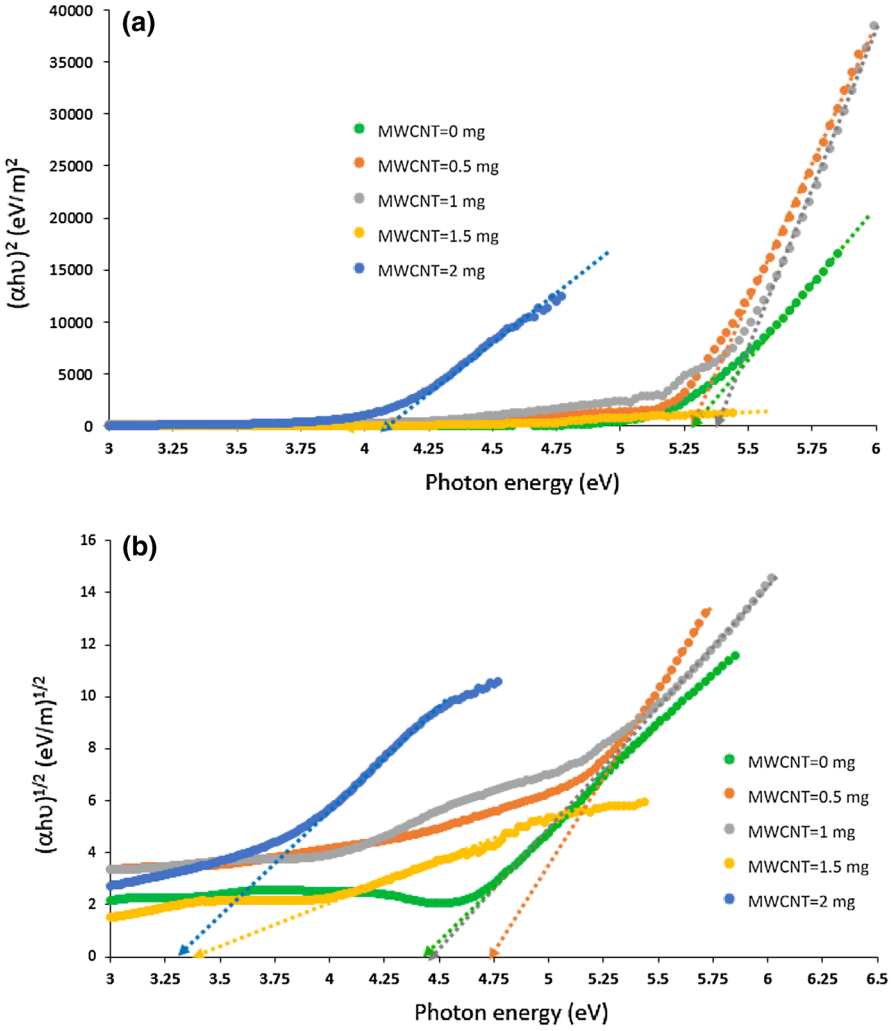

Fig. 4 Tauc plots of Gelatin/PAAm/MWCNT composites with various MWCNT amounts: 0, 0.5, 1, 1.5, 2 mg for **a** direct, **b** indirect allowed transitions

Table 2 shows that resonance ratio values are higher than other MWCNT amounts and normalized width values are low enough to indicate good dispersion in the composite materials. High resonance ratio and low normalized width ratio provide good dispersion for the single-wall carbon nanotubes [46]. This approach is likely to result in high resonance ratio and low normalized width ratio conditions for proving the well-dispersed composites [25]. Sonication process is the main contribution that maintains the good dispersion of the MWCNTs inside the polymeric matrix.

When the amount of MWCNT is increased somewhat more (the amount of MWCNT is 1.5 mg), the maximum absorbance intensity value decreases sharply.

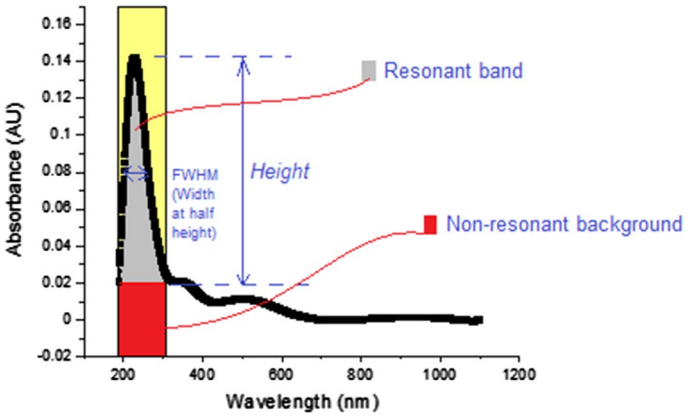

Fig. 5 Absorbance–wavelength curve of Gelatin/PAAm/MWCNT composite with MWCNT amount of 1.5 mg indicating the parameters that prove the good dispersion of doping materials inside composites

The absorbance peak becomes wider and shifts toward the long wavelength (red-shifted). The weakening and broadening of the absorbance peaks could be attributed to the increase of the scattering due to MWCNTs. There is an increase in the resonance ratio and the normalized width exhibits an exponential increase. As the amount of MWCNT increases, the composite material is expected to be less transparent. Although the amount of MWCNT increases, while the absorbance intensity value is expected to increase, its decrease can be interpreted as the MWCNTs in the composite material not being localized sufficiently in the gelatin / PAAm environment, i.e., not being connected to this network, suspending in the liquid homogeneously, and increasing scattering intensity. It is not surprising that the sum of absorbance and transmittance data does not meet with 1 because of the scattering. On the other hand, the decrease in the absorbance intensity value indicates that the MWCNTs are better distributed in the composite matrix and there is no agglomeration. The increase in the resonance ratio (see Table 2) also confirms the better dispersion of MWCNT inside the composite material. However, the normalized width value increases dramatically.

The increase in the amount of MWCNT (to 2 mg) promotes the opacity, which leads to the increase in the absorbance intensity. When the amount of MWCNT in the composite is increased from 1.5 mg to 2 mg, the resonance ratio value increases. On the other hand, the value of the normalized width is lower than calculated for 1.5 mg of MWCNT. This is a sign that the doping material in the composite is better dispersed. Figure 7 summarizes the results for the resonance ratio and normalized width. It is obvious to see that the optimum amount of MWCNT to obtain a well-dispersed solution is 2 mg, since it has the highest resonance ratio and the normalized width is sufficiently low.

Further increase in MWCNT amount leads to reach PDI values higher than 0.5 which are considered to be associated with polydisperse/nonhomogeneously distributed samples as reported earlier [36]. Therefore, the composites containing MWCNT more than 2.0 mg have not been investigated.

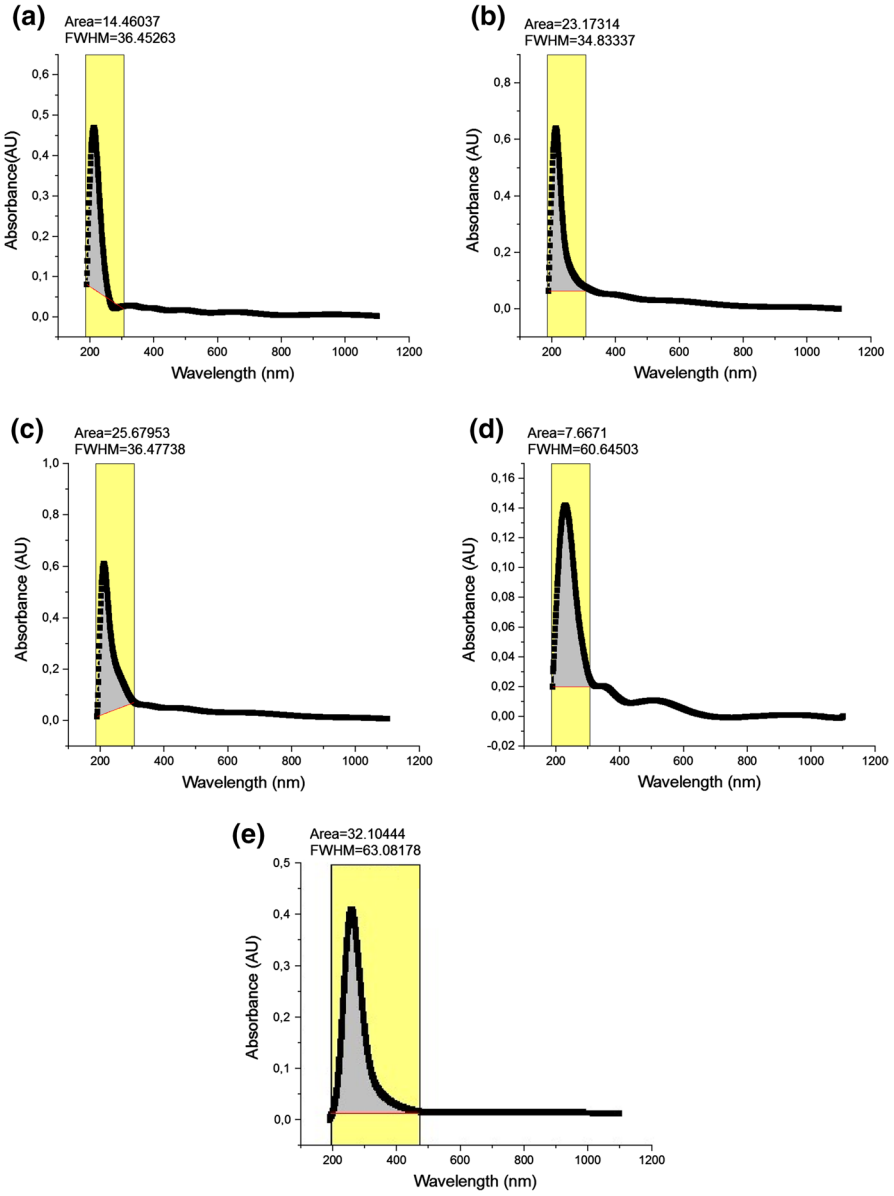

Fig. 6 Absorbance–wavelength curves of Gelatin/PAAm/MWCNT composites with various MWCNT amounts: **a** 0 mg, **b** 0.5 mg, **c** 1 mg, **d** 1.5 mg, **e** 2 mg. Area represents the area of the resonant band and FWHM represents width at half-height

Conclusion

Well-dispersed multiwalled carbon nanotube (MWCNT) and gelatin-enhanced polyacrylamide (PAAm) composites were synthesized via a surfactant-free free-radical

Table 2 Resonance ratio and normalized width values of composites with various MWCNT amounts revealing whether the doping materials in composite materials are well-dispersed

MWCNT amount in Gelatin/PAAm/MWCNT composite (mg)	Area of resonant band	Area of nonresonant background	Resonance Ratio	Width of resonant band	Height of resonant band	Normalized width
0	14.460	11.729	**1.233**	36.453	0.400	**91.106**
0.5	23.173	19.183	**1.208**	34.833	0.575	**60.556**
1	25.679	16.877	**1.521**	36.477	0.582	**62.619**
1.5	7.667	4.686	**1.636**	60.645	0.122	**498.070**
2	32.104	18.828	**1.705**	63.082	0.434	**145.433**

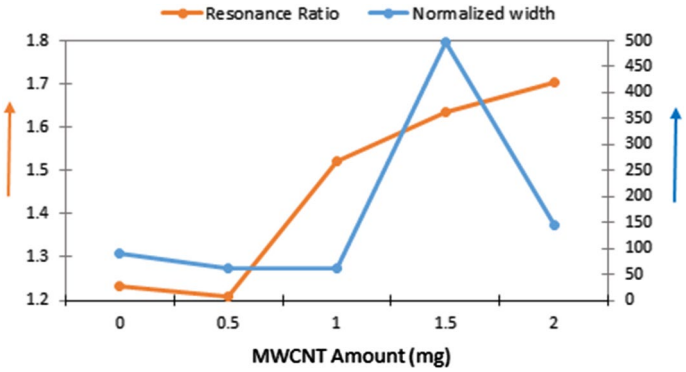

Fig. 7 Calculated resonance ratio and normalized width of Gelatin/PAAm/MWCNT composites with various MWCNT amounts: 0, 0.5, 1, 1.5, 2 mg

copolymerization method. MWCNTs were added to the composite mixture in various amounts (0.5 mg, 1.0 mg, 1.5 mg, and 2.0 mg) during the nucleation process in order to increase the conductivity. The increase in the amount of MWCNT promotes the opacity, which leads to the increase in the absorbance intensity. It is worth mentioning that sonication process is the main contribution to maintain the good dispersion of the MWCNTs inside the polymeric matrix lowering the normalized width and increasing the resonance ratio. Realizing the proper ultra-sonication method resulted in good dispersion of nanotubes. High resonance ratio and low normalized width ratio conditions for proving the well-dispersed composites have been obtained for composite with MWCNT amount of 2 mg. Furthermore, loading high concentrations of MWCNT to composites caused a significant decrease in the bandgap energy of the composites. Bandgap energy of composites can be tuned by controlling the MWCNT amount. These composites can prevent UV-induced lipid peroxidation and postpone the oxidation caused by light in food and biomedical applications. Also, such biocompatible polymeric matrix reinforced with MWCNT composite materials can be used as a structural material for implants, compounds of biological tissues, artificial muscles, and packaging materials.

References

1. Gerasimenko AY, Ichkitidze LP, Podgaetsky VM, Selishchev SV (2015) Biomedical applications of promising nanomaterials with carbon nanotubes. Biomed Eng 48:310–314. https://doi.org/10.1007/s10527-015-9476-z
2. Begum P, Ikhtiari R, Fugetsu B (2014) Potential impact of multi-walled carbon nanotubes exposure to the seedling stage of selected plant species. Nanomaterials 4:203–221. https://doi.org/10.3390/nano4020203
3. Stout DA, Webster TJ (2012) Carbon nanotubes for stem cell control. Mater Today 15:312–318. https://doi.org/10.1016/S1369-7021(12)70136-0
4. Maiti D, Tong X, Mou X, Yang K (2018) Carbon-based nanomaterials for biomedical applications: a recent study. Front Pharmacol 9:1401. https://doi.org/10.3389/fphar.2018.01401

5. Silversmith EF (1992) Free-radical polymerization of acrylamide. J Chem Educ 69(9):763. https://doi.org/10.1021/ed069p763.1
6. Okaiyeto K, Nwodo UU, Okoli SA, Mabinya LV, Okoh AI (2016) Implications for public health demands alternatives to inorganic and synthetic flocculants: bioflocculants as important candidates. Microbiologyopen 5(2):177–211. https://doi.org/10.1002/mbo3.334
7. Banga JP (1998) Encyclopedia of immunology, 2nd edn. Academic Press, pp 2143–2144. https://www.elsevier.com/books/encyclopedia-of-immunology/9780122267659
8. Christensen LH, Breiting VB, Aasted A, Jørgensen A, Kebuladze I (2003) Long-term effects of polyacrylamide hydrogel on human breast tissue. Plast Reconstr Surg 111(6):1883–1890. https://doi.org/10.1097/01.PRS.0000056873.87165.5A
9. Vasile C, Pamfil D, Stoleru E, Baican M (2020) New developments in medical applications of hybrid hydrogels containing natural polymers. Molecules 25(7):1539. https://doi.org/10.3390/molecules25071539
10. Anderson JM (1986) Polymeric biomaterials. Martinus Nijhoff Publishers, Boston, pp 29–39
11. Serrano MC, Pagani R, Vallet-Regí M, Peña J, Rámila A, Izquierdo I, Portolés MT (2004) In vitro biocompatibility assessment of poly (ε-caprolactone) films using L929 mouse fibroblasts. Biomaterials 25:5603–5611
12. Akiyama Y, Kikuchi A, Yamato M, Okano T (2014) Accelerated cell-sheet recovery from a surface successively grafted with polyacrylamide and poly(N-isopropylacrylamide). Acta Biomaterialia 10(8):3398–3408. https://doi.org/10.1016/j.actbio.2014.03.024
13. Jeon IY, Baek JB (2010) Nanocomposites derived from polymers and inorganic nanoparticles. Materials 3:3654–3674. https://doi.org/10.3390/ma3063654
14. Madni I, Hwang CY, Park SD, Choa YH, Kim HT (2010) Mixed surfactant system for stable suspension of multiwalled carbon nanotubes. Colloids Surf A: Physicochem Eng Asp 358(1–3):101–107. https://doi.org/10.1016/j.colsurfa.2010.01.030
15. Xie XL, Mai YW, Zhou XP (2005) Dispersion and alignment of carbon nanotubes in polymer matrix: a review. Mater Sci Eng R: Rep 49(4):89–112. https://doi.org/10.1016/j.mser.2005.04.002
16. Ishaq A, Sobia AR, Yan L (2010) Effect of ion irradiation on the properties of carbon nanotube buckypapers. J Exp Nanosci 5(3):213–220. https://doi.org/10.1080/17458080903465162
17. Kim Y, Torrens ON, Kikkawa JM, Abou-Hamad E, GozeBac C, Luzzi DE (2007) High-purity diamagnetic single-wall carbon nanotube buckypaper. Chem Mater 19(12):2982–2986. https://doi.org/10.1021/cm063006h
18. Grossiord N, Loos J, Van Laake L, Maugey M, Zakri C, Koning CE, Hart AJ (2008) High-conductivity polymer nanocomposites obtained by tailoring the characteristics of carbon nanotube filers. Adv Func Mater 18(20):3226–3234. https://doi.org/10.1002/adfm.200800528
19. Bahr JL, Yang J, Kosynkin DV, Bronikowski MJ, Smalley RE, Tour JM (2001) Functionalization of carbon nanotubes by electrochemical reduction of aryl diazonium salts: a bucky paper electrode. J Am Chem Soc 123(27):6536–6542. https://doi.org/10.1021/ja010462s
20. McNally T, Pötschke P (eds) (2011) Polymer-carbon nanotube composites: preparation, properties and applications. Elsevier. https://www.elsevier.com/books/polymer-carbon-nanotube-composites/mcnally/978-1-84569-761-7
21. Huang YY, Terentjev EM (2012) Dispersion of carbon nanotubes: mixing, sonication, stabilization, and composite properties. Polymers 4(1):275–295. https://doi.org/10.3390/polym4010275
22. Ma P-C, Siddiqui NA, Marom G, Kim J-K (2010) Dispersion and functionalization of carbon nanotubes for polymer-based nanocomposites: a review. Compos A Appl Sci Manuf 41(10):1345–1367. https://doi.org/10.1016/j.compositesa.2010.07.003
23. Atif R, Inam F (2016) Reasons and remedies for the agglomeration of multilayered graphene and carbon nanotubes in polymers. Beilstein J Nanotechnol 7:1174–1196. https://doi.org/10.3762/bjnano.7.109
24. LiaoY-H M-T, Liang Z, Zhang C, Wang B (2004) Investigation of the dispersion process of SWNTs/SC-15 epoxy resin nanocomposites. Mater Sci Eng, A 385(1–2):175–181. https://doi.org/10.1016/j.msea.2004.06.031
25. Njuguna J, Vanli OA, Liang RA (2015) Review of spectral methods for dispersion characterization of carbon nanotubes in aqueous suspensions. J Spectrosc 463156:1–11. https://doi.org/10.1155/2015/463156
26. Islam T, Salem KS, Biswas S, Haque P, Rimu SH, Rahman MM (2018) Preparation of carbon nanotube reinforced gelatin-chitosan- hydroxyapatite biocomposite for bone tissue engineering. Open Access J Biomed Eng Biosci 1(3):66–72

27. Kavoosi G, Dadfar SMM, Dadfar SMA, Ahmadi F, Niakosari M (2014) Investigation of gelatin/multi-walled carbon nanotube nanocomposite films as packaging materials. Food Sci Nutr 2(1):65–73. https://doi.org/10.1002/fsn3.81
28. Sun X, Qin Z, Ye L, Zhang H, Yu Q, Wu X, Li J, Yao F (2020) Carbon nanotubes reinforced hydrogel as flexible strain sensor with high stretchability and mechanically toughness. Chem Eng J 382:122832. https://doi.org/10.1016/j.cej.2019.122832
29. Gorgieva S, Kokol V (2011) Collagen-vs. gelatine-based biomaterials and their biocompatibility: review and perspectives. Biomaterials applications for nanomedicine. InTech. https://www.intechopen.com/books/biomaterials-applications-for-nanomedicine/collagen-vs-gelatine-based-biomaterials-and-their-biocompatibilityreview-and-perspectives
30. Lai JY (2010) Biocompatibility of chemically cross-linked gelatin hydrogels for ophthalmic use. J Mater Sci: Mater Med 21:1899–1911. https://doi.org/10.1007/s10856-010-4035-3
31. Yang G, Xiao Z, Long H et al (2018) Assessment of the characteristics and biocompatibility of gelatin sponge scaffolds prepared by various crosslinking methods. Sci Rep 8:1616. https://doi.org/10.1038/s41598-018-20006-y
32. Yi F-L, Meng F-C, Li Y-Q, Huang P, Hu N, Liao K, Fu S-Y (2020) Highly stretchable CNT Fiber/PAAm hydrogel composite simultaneously serving as strain sensor and supercapacitor. Eng Comp Part B 198:108246. https://doi.org/10.1016/j.compositesb.2020.108246
33. Cao N, Yang X, Fu Y (2009) Effects of various plasticizers on mechanical and water vapor barrier properties of gelatin films. Food Hydrocoll 23:729–735. https://doi.org/10.1016/j.foodhyd.2008.07.017
34. Gomez-Guillen MC, Gimenez B, Lopez-Caballero ME, Montero MP (2011) Functional and bioactive properties of collagen and gelatin from alternative sources. Food Hydrocoll 25:1813–1827. https://doi.org/10.1016/j.foodhyd.2011.02.007
35. Dassios KG, Alafogianni P, Antiohos SK, Leptokaridis C, Barkoula NM, Matikas TE (2015) Optimization of sonication parameters for homogeneous surfactant-assisted dispersion of multiwalled carbon nanotubes in aqueous solutions. J Phys Chem C 119(13):7506–7516. https://doi.org/10.1021/acs.jpcc.5b01349
36. Alafogianni P, Dassios K, Farmaki S, Antiohos SK, Matikas TE, Barkoula NM (2016) On the efficiency of UV–vis spectroscopy in assessing the dispersion quality in sonicated aqueous suspensions of carbon nanotubes. Coll Surf: Physicochem Eng Asp 495:118–124. https://doi.org/10.1016/j.colsurfa.2016.01.053
37. International Union of Pure and Applied Chemistry-IUPAC (1997) Compendium of Chemical Terminology, 2nd edn. (the "Gold Book"). Compiled by A. D. McNaught and A. Wilkinson. Blackwell Scientific Publications, Oxford Online version (2019-) https://doi.org/https://doi.org/10.1351/goldbook.
38. Jiang L, Gao L, Sun J (2003) Production of aqueous colloidal dispersions of carbon nanotubes. J Colloid Interface Sci 260(1):89–94. https://doi.org/10.1016/S0021-9797(02)00176-5
39. Ahmad M, Benjakul S, Prodpran T, Agustini TW (2012) Physico-mechanical and antimicrobial properties of gelatin film from the skin of unicorn leatherjacket incorporated with essential oils. Food Hydrocoll 28:189–199. https://doi.org/10.1016/j.foodhyd.2011.12.003
40. Voge CM, Johns J, Raghavan M, Morris MD, Stegemann JP (2013) Wrapping and dispersion of multi-walled carbon nanotubes improves electrical conductivity of protein-nanotube composite biomaterials. J Biomed Mater Res A 101:231–238. https://doi.org/10.1002/jbm.a.34310
41. Garrido T, Penalba M, de la Caba K, Guerrero P (2016) Injection-manufactured biocomposites from extruded soy protein with algae waste as a filler. Compos B 86:197–202. https://doi.org/10.1016/j.compositesb.2015.09.058
42. Ohring M (2002) Materials science of thin films: epitaxy, 2nd edn. Academic Press, pp 417–494. https://www.sciencedirect.com/book/9780125249751/materials-science-of-thin-films
43. Kittel C (2004) Introduction to solid state physics, 8th edn. Wiley. https://www.wiley.com/en-us/Introduction+to+Solid+State+Physics%2C+8th+Edition-p-9780471415268
44. Soroush M, Lau KK (eds) (2019) Dye-sensitized solar cells: mathematical modelling, and materials design and optimization. Academic Press, pp 51–81. https://www.sciencedirect.com/book/9780128145418/dye-sensitized-solar-cells
45. Tauc J (1968) Optical properties and electronic structure of amorphous Ge and Si. Mater Res Bull 3:37–46. https://doi.org/10.1016/0025-5408(68)90023-8
46. Tan Y, Resasco DE (2005) Dispersion of single-walled carbon nanotubes of narrow diameter distribution. J Phys Chem B 109(30):14454–14460. https://doi.org/10.1021/jp052217r